J. Membrane Biol. 135, 165–180 (1993)

The Journal of
Membrane
Biology

Double Whole-Cell Patch-Clamp Characterization of Gap Junctional Channels in Isolated Insect Epidermal Cell Pairs

Dennis Churchill, Stanley Caveney
Department of Zoology, University of Western Ontario, London, Ontario, Canada, N6A 5B7

Received: 11 January 1993/Revised: 12 April 1993

Abstract. Double whole-cell patch-clamp methods were used to characterize junctional membrane conductances in epidermal cell pairs isolated from the prepupal integument of the flour beetle, *Tenebrio molitor*. The mean initial junctional conductance in 267 cell pairs was 9.5 ± 1.0 nS (range 0–95 nS). Well-coupled cell pairs uncoupled spontaneously with a half-time of 7.6 min. Adding 5 mM ATP to the pipette solution stabilized coupling with less than a 50% drop occurring after 30 min. Nonjunctional membrane potential was the major determinant of junctional conductance with transjunctional potential playing a minor role. Junctional conductance approached 0 pA at nonjunctional membrane potentials greater than 0 mV and increased with hyperpolarization. The voltage at half-maximal conductance was −26 mV. The time course of the reversible changes in junctional conductance were slow (≤30 sec) with time-dependent decay occurring faster and recovery occurring slower with increasing depolarization. Single gap junctional channel activity was recorded in uncoupling cell pairs and in poorly coupled ATP-stabilized cell pairs. One main single channel conductance was observed in each cell pair. The mean single channel conductances from all cell pairs in this study ranged from 197–347 pS (mean 248 pS). Single channel conductance was linear over the ±60 mV transjunctional voltage range tested. A broad range of subconductance states of the main state representing 5% of the total open time of measurable main state events was observed. Single channel activity was strongly dependent on the nonjunctional membrane potential, increasing with hyperpolarization.

* *Correspondence to:* S. Caveney

Key words: Gap junctions — Patch-clamp — Epidermis — *Tenebrio molitor* — Single channels — Voltage dependence

Introduction

A cellular monolayer, the epidermis, is responsible for the external morphological changes that occur during insect growth and metamorphosis (Wigglesworth, 1984). To perform complex spatial tasks, the cells of the epidermis must coordinate their activities through some form of intercellular communication. As gap junctions are present in developing tissues, it has been suggested that they mediate cell-to-cell interactions during development (*for reviews see* Caveney, 1985; Guthrie & Gilula, 1989). Each insect epidermal cell is coupled to its immediate neighbors by tens of thousands of gap junctional channels (Berdan & Caveney, 1985) which allow the cells to share inorganic ions and small organic metabolites of up to 2,000 D (*reviewed in* Loewenstein, 1981; Bennett et al., 1991). These cytoplasmic metabolites could include signal molecules capable of coordinating cell function during development (Wolpert, 1978).

Several observations on intact integument (epidermis plus cuticle) suggest that gap junctions play a significant role during epidermal growth. Junctional ionic conductance climbs as the segment grows in size (Caveney & Safranyos, 1989) and also fluctuates in a predictable pattern during the molt cycle (Caveney, 1978). Exposing the epidermis to the developmental hormone 20-hydroxyecdysone *in vitro* caused an increase in junctional permeability to inorganic ions (Caveney & Blennerhassett, 1980) but not to fluorescent tracers (Caveney & Safranyos, 1989). Some of these developmental changes in junctional

permeability in the epidermal segment appear to involve the gating of gap junctional channels and not an increase in their synthesis or deployment in the plasma membrane (Berdan & Caveney, 1985; Caveney, Berdan & McLean, 1980). In addition, the gap junctions in strips of cells at segment boundaries have reduced permeability to fluorescent tracers but not to inorganic ions, and thus establish communication compartments in the epidermis (Warner & Lawrence, 1982; Blennerhassett & Caveney, 1984; Ruangvoravat & Lo, 1992). These observations raise two questions that are difficult to address in the intact epidermis, namely (i) how are epidermal gap junctional channels gated, and (ii) how is the macroscopic permeability to ions and small organic molecules (permselectivity) regulated discoordinately? Are there channels with different permeabilities or channel substates with distinct permeability characteristics?

In the present study, we have begun to address the first question using the double whole-cell patch-clamp method (Neyton & Trautmann, 1985; Veenstra & DeHaan, 1986). When applied to small cells, this method allows the voltage dependence of gap junctions and the properties of single channels to be determined. The modulation of channel gating by cytoplasmic metabolites can be assessed by including them in the pipette solution (e.g., Neyton & Trautmann, 1986; Somogyi & Kolb, 1988). Only one patch-clamp study and two conventional voltage-clamp studies on insect cell pairs have been reported (Obaid, Socolar & Rose, 1983; Verselis, Bennett & Bargiello, 1991; Bukauskas, Kempf & Weingart, 1991). In each case, junctional conductance was found to be strongly dependent on the nonjunctional membrane potential (V_M). V_M-dependent gating is rarely observed in vertebrate cell types in which voltage-dependent gating depends strictly on transjunctional voltage (V_J) (extensively reviewed by Spray & Bennett, 1985; Spray et al., 1991*a*). V_J dependence is usually symmetric about V_J = 0 mV (e.g., Veenstra, 1990; Wang et al., 1992) but may be asymmetric as in the rectifying synapses of invertebrate giant axons (e.g., Giaume, Kado & Korn, 1987). Another distinction between typical insect and vertebrate junctions is the larger apparent limiting pore size of the channels in insects (Flagg-Newton, Simpson & Loewenstein, 1979; Schwarzmann et al., 1981; Zimmerman & Rose, 1985).

We report here a patch-clamp analysis of dissociated epidermal cell pairs for the larva of the beetle *T. molitor*. The junctional membrane conductance in well-coupled cell pairs, its voltage dependence and stabilization by adding ATP to the pipette solution are described. The properties of single gap junctional channels in poorly coupled cell pairs including voltage dependence, conductances of the main state (γ_J) and its substates are also presented. A preliminary report based on some of these data has appeared elsewhere (Churchill & Caveney, 1993*a*).

Materials and Methods

Cell Preparation

Cell preparation is as previously described in Churchill and Caveney (1993*b*). Abdominal segments were excised from 6–10 prepupae of the flour beetle *T. molitor* (anesthetized by submersion in 70% ethanol for 4 min) following apolysis (natural detachment of the epidermis from the cuticle) and placed into *Tenebrio* bath saline ('TBS'; in mM: 80 NaCl, 43 KCl, 3 $CaCl_2$, 10 $MgCl_2$, 90 sucrose, 10 glucose, 20 PIPES; pH 6.7 with 1 M NaOH). The fat body was teased away from the epidermis, which remained loosely attached to the cuticle through muscle attachments. Following dissection, the tissue was placed into 1 ml of 0.2–0.4% collagenase (type IA) or 0.1% pronase E (type XXV; Sigma, St. Louis, MO; stored at −20°C as 1% stocks in TBS and diluted in TBS for use) and incubated for 10–20 or 1–5 min for collagenase and pronase, respectively. This was then diluted with TBS, gently triturated 1–3 times with a pasteur pipette (4 mm diameter opening) and washed twice by centrifuging at 100 × *g* and resuspending in TBS. Cells were then plated on a glass coverslip fixed in an acrylic superfusion chamber. The spherical (10–15 μm diameter) epidermal cells were allowed to adhere to the glass substrate for 30–60 min before use. Five to thirty healthy cell pairs were isolated using this procedure. Isolation was carried out at 24–28°C.

Electrophysiological Methods

Once adherent to the coverslip, the epidermal cells were superfused with 5–10 ml of TBS and frequently superfused with TBS throughout the experiment. All experiments were performed on paired spherical epidermal cells at 24–28°C within 8–10 hr of isolation using standard double whole-cell patch-clamp techniques (Neyton & Trautmann, 1985; Rook, Jongsma & van Ginneken, 1988; Veenstra & DeHaan, 1988; Giaume, 1991; Churchill et al., 1993). Patch pipettes of 2–8 MΩ resistance filled with a conventional pH 6.7 *Tenebrio* pipette solution (in mM: 100 KCl, 10 NaCl, 1 $CaCl_2$, 2 $MgCl_2$, 10 EGTA/45 KOH (added from a 50 mM EGTA/225 mM KOH stock solution), 20 PIPES, 80 sucrose; pH 6.7 with 1 M KOH) were used. For ATP experiments, 5 mM Na_2-ATP was added to the pipette solution before adjusting the pH. Stray capacitance was reduced by coating pipette tips with pure white beeswax (Fisher Scientific, Toronto). Pipettes were attached to the head stages of two, independent List L/M EPC-7 patch-clamp amplifiers (Medical Systems, New York). Digital records were stored to VCR tape using a 4-channel pulse code modulator (PCM) with a sampling frequency of 22 kHz (Medical Systems, New York) and to the hard disk of an IBM compatible 386 computer using a 125 kHz TL-1 DMA AD/DA interface (Axon Instruments, Foster City, CA). In-house software designed for double whole-cell recording (Axobasic, Axon) or pCLAMP (Axon) was used to set stimulation and acquisition parameters. Data were filtered upon playback from VCR tape at 0.2 × sample frequency using an analog 8-pole low-pass Bessel

filter (Frequency Devices, Haverhill, MA). Giga-ohm seals of 5–60 GΩ on the cell were formed with a success rate > 90% ($n > 200$). Upon rupture (mouth suction) of the membrane patch in each pipette (break-in) capacitive current spikes in both cells were monitored using simultaneous square voltage pulses to −60 mV from holding voltages (V_H) of −50 mV. Capacitive currents were stored to disk (sample frequency = 42 kHz) for off-line analysis using pCLAMP (Axon). Capacitance and series resistance (R_S) compensation circuitry was not used so that R_S could be monitored rapidly throughout the experiment. Series resistance (R_S) was estimated by dividing the change in pipette voltage (10 mV) by the peak of the capacitive current. The values of R_S, whole-cell capacitances and membrane potentials just after break-in in 54 cell pairs (n = 108 cells) were 19.9 ± 0.9 MΩ (10–38 MΩ), 9.8 ± 0.5 pF (5–16 pF) and −20 to −60 mV. All voltages are expressed as inside negative.

All averaged data are expressed as mean ± SEM unless stated otherwise.

Junctional Conductance Calculation

Measurement of macroscopic currents (I_J), calculation of junctional conductance (G_J), and correction for series resistance errors have already been described in detail (Neyton & Trautmann, 1985; Rook et al., 1988; Veenstra & DeHaan, 1988; Giaume, 1991). In experiments in which G_J was not corrected for R_S errors, G_J was calculated by dividing I_J by V_J, where V_J is the voltage difference between cell 1 and cell 2 during a square voltage pulse ($V_J = V_1 - V_2$) and I_J is the absolute change in current in the nonpulsed cell (i.e., I_1 or I_2). For R_S correction G_J was calculated with the equation

$$G_J = I_J/\{V_J - (R_{S1} * I_1 - R_{S2} * I_2)\},$$

where R_{S1} and R_{S2} are R_S for cell 1 and cell 2, respectively. R_S in 14 cell pairs changed an average of 56% in 20 min during voltage-dependence experiments.

Open-close events of single gap junctional channels in poorly coupled cells ($G_J < 1.5$ nS) were recognized as spontaneous step-like transitions in the current signals of both cells which were equal in magnitude but opposite in polarity (with V_J held constant at 20 or 10 mV). Single channel conductances (γ_J) were measured for the trace with the higher signal-to-noise ratio. The magnitude of the single channel current (Δi_J) was measured by visually averaging the plateau of the current transitions using the vertical cursors of Axotape (Axon Instruments). Frequency histograms of these events were constructed by grouping the calculated conductances ($\gamma_J = \Delta i_J/V_J$) of all step-like transitions from one cell pair into bins. These distributions were fitted to single Gaussian curves using the Gaussian-Newton approximation algorithm of pCLAMP (Axon). Data were acquired from tape to disk for analysis by sampling at 500 Hz and filtering at 100 Hz. Series resistance errors for γ_J measurements were ≪10%.

Results

Spontaneous Uncoupling and Stabilization of Coupling by ATP

The mean initial G_J in 267 cell pairs was 9.5 ± 1.0 nS ranging from 0–95 nS. In 4% of these, single channel activity was observed immediately after break-in; 24% of the pairs were completely uncoupled. For these measurements the potentials of both cells were held at −50 mV (i.e., V_H = −50 mV) and depolarizing 20 mV pulses were applied to one cell or hyperpolarizing 20 mV pulses were applied alternately to both cells. Well-coupled cell pairs rapidly uncoupled following break-in when ATP-free pipette solution was used (Fig. 1*A*). As I_J dropped and the amplifier gains were increased, open-close events of single gap junctional channels were detectable as spontaneous and quantal changes in the recorded currents (I_1 and I_2) that were equal in magnitude but opposite in sign (Figs. 1*A* and 2). To observe single channel activity, the pulsing was stopped and V_J set at a constant level. Channel activity lasted < 10 min once detected. The mean half-time to uncoupling (to the level of single channels) for 12 cell pairs (with initial $G_J > 10$ nS) was 7.6 min (Fig. 1*B*).

Since "rundown" of G_J (i.e., spontaneous uncoupling) has been explained in other cell types to be due to washout (Neyton & Trautmann, 1986; Somogyi & Kolb, 1988), the effect of ATP in the pipette on G_J was tested. Washout occurs when the pipette solution dilutes soluble cytoplasmic components (Pusch & Neher, 1988). ATP (5 mM) in the pipette solution substantially inhibited rundown with G_J, slowly decreasing to less than 50% in 30 min (Fig. 1*B*). G_J often increased within minutes of break-in, suggesting that 5 mM ATP may have been higher than endogenous levels in those cells. G_J in well-coupled ATP-loaded cell pairs never dropped to the single channel level. In four cell pairs the initial G_J was < 2 nS and single channel events were observable immediately after break-in.

Single Channel Properties

Poorly coupled ATP-loaded cell pairs were used for most of the analysis of unitary channel conductance (γ_J) since more events were available for any single cell pair than from non-ATP-loaded cell pairs. The length of single channel recording and the number of events per cell pair for ATP-loaded and non-ATP-loaded cell pairs were, respectively: 16.25 ± 1.57 min (n = 4 cell pairs) *vs.* 6.05 ± 0.93 min (n = 14 cell pairs) and 270 ± 70 *vs.* 104 ± 20 observable events per cell pair (not necessarily all events were measurable).

Main Conductance State

Upon visual inspection of channel data from any cell pair, it was clear that there was only one main conductance state (Figs. 2 and 3*A*). Also, during the

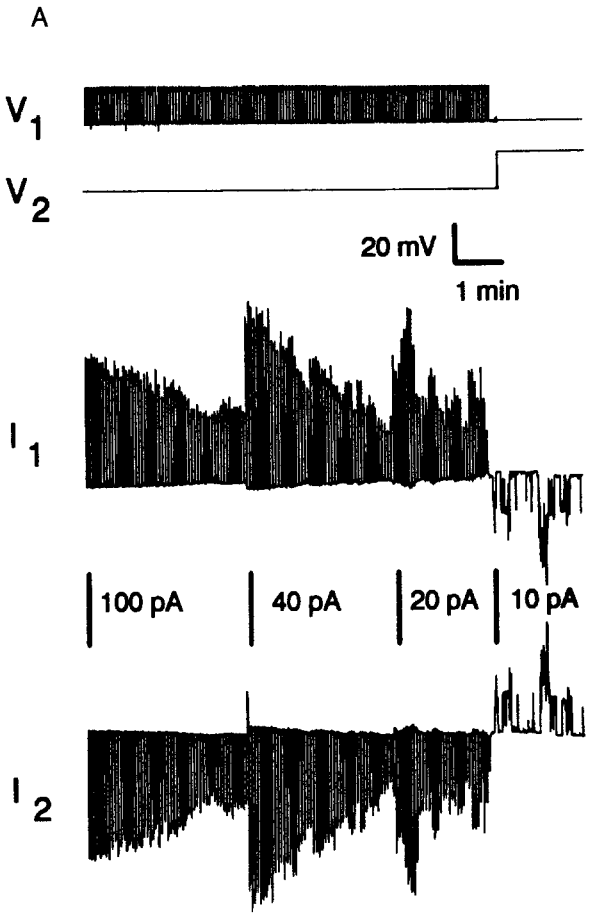

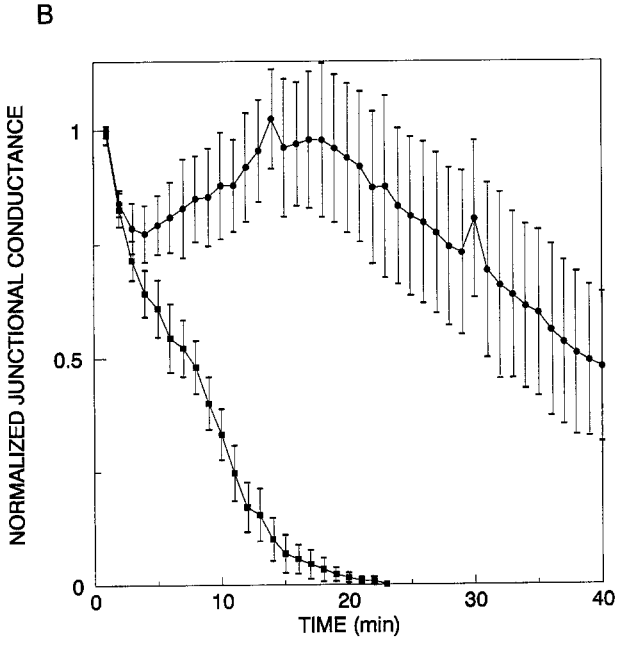

Fig. 1. Spontaneous uncoupling and stabilization of junctional conductance by 5 mM ATP in the pipette solution. (*A*) Current (I_1 and I_2) and voltage (V_1 and V_2) traces are shown (compressed time scale) from a cell pair without ATP in the pipette solution. Voltage pulses (1 sec, 20 mV, 0.3 Hz) were applied to cell 1 with $V_H = -50$ mV for both cells. Bars between the current traces indicate changes in amplifier gain. Initial $I_J = 180$ pA ($G_J = 9$ nS) declined to the 5 pA current ($\gamma_J = 250$ pS) representative of single channels within 10 min. A constant V_J with a reversed polarity of 20 mV ($V_1 = -50$ mV, $V_2 = -30$ mV) was used to monitor the spontaneous and quantal behavior of the single channel events at the end of the current traces. The data for the figure were sampled from tape at 15 Hz. (*B*) G_J (I_J/V_J) from 12 cell pairs without ATP in the pipette were normalized to the initial G_J and graphed against time after break-in (■). Data points at one-min intervals are shown. Cell pairs rapidly uncoupled with a half-time to unitary channel events of 7.6 min. When 5 mM ATP was added to the pipette solution, spontaneous uncoupling was inhibited (●). G_J gradually decreased with time but never to the conductance level at which unitary channels events were observed ($n = 8$ cell pairs). The initial G_J was > 10 nS in all cell pairs.

open period of the main state, substates of smaller conductance were observed (Fig. 4*A a* and *d*). Main state and substate conductances were analyzed separately. To analyze main state conductance, all main state transitions were measured from one cell pair and grouped into 7 pS bins on a frequency histogram (Fig. 3*A*). The distribution in Fig. 3*A* approximated a normal distribution and was fit with a single Gaussian curve with a mean ± SD of 197.21 ± 13.39 pS ($n = 492$ events). From two other cell pairs (with $n > 100$) the mean ± SD for a best fit single Gaussian curve were 214.72 ± 42.05 pS ($n = 287$ events) and 293.46 ± 24.24 pS ($n = 166$ events). The arithmetic mean conductance for 169 single level channel events from 13 spontaneously uncoupled cell pairs was 288.68 ± 2.42 pS (mean ± SEM), ranging from individual cell pair means of 260.56 ± 8.83 pS ($n = 9$ events) to 347 ± 3.84 pS ($n = 4$ events).

The V_J dependence of the single channel current (i_J) was determined using spontaneously uncoupled cells (ATP-free pipette) since it was easier to obtain data from several pairs. One cell was clamped at 0 mV and the other at a range of voltages between 0 to −60 mV. Reversal of i_J was obtained by alternating the cell clamped at 0 mV. The single channel *I-V* relationship is shown in Fig. 3*B* for data obtained from six cell pairs. This was fit with a regression line of slope 271 ± 0.01 pS ($r^2 = 0.99$) using a linear least-squares method. Typical single channel events from which these measurements were made are shown in Fig. 3*C* for $V_J = +40$ to −40 mV. From these results we conclude that over the voltage range tested, and for the periods of time that channel activity was observed at each V_J (~1 min), the main state i_J *vs.* V_J is ohmic.

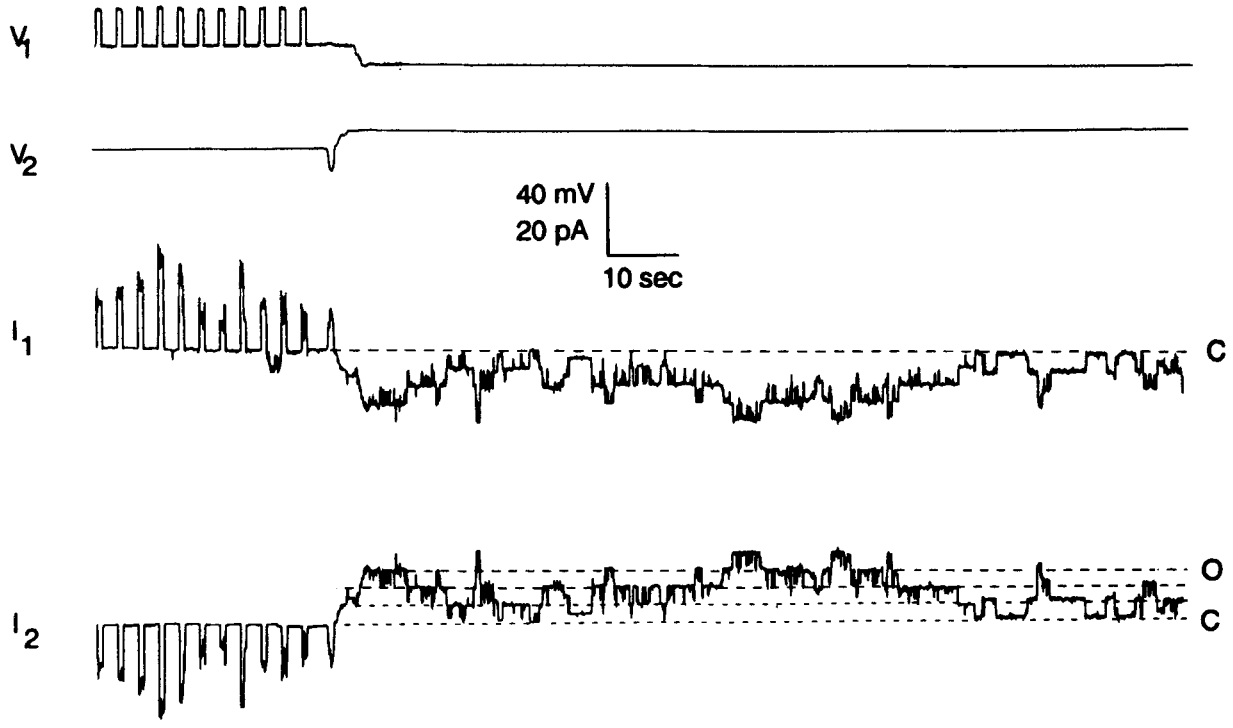

Fig. 2. Unitary currents from single gap junctional channels observed in a poorly coupled cell pair following spontaneous uncoupling. Current (I_1 and I_2) and voltage (V_1 and V_2) traces are shown on an expanded time scale from a cell pair clamped with pipettes containing an ATP-free solution. A train of voltage pulses (1 sec, 20 mV, 0.3 Hz) was initially applied to cell 1 with $V_H = -50$ mV for both cells. A constant V_J with a reversed polarity of 20 mV ($V_1 = -60$ mV, $V_2 = -40$ mV) was used to monitor the spontaneous and quantal behavior of the unitary single channel currents. Each dotted line represents 4.6–5 pA (230–250 pS) of conductance. Baseline (closed) is indicated at *C*. *O* indicates the direction of channel opening. The data for this figure were sampled from tape at 100 Hz.

In four ATP-loaded cell pairs the open duration of main state events was measured. Only single channel events opening from the baseline (closed) and uninterrupted by openings of other channels were selected for these measurements. Open durations ranged from 14 msec to 13.3 sec for a mean of 753 ± 101 msec (n = 189 events). In one typical ATP-loaded cell pair the transition times between the fully open state and baseline were measured for 52 smooth transitions (sample frequency = 5 kHz). Transition times ranged from 0.4–28.8 msec with a mean of 5.40 ± 0.97 msec. The mean transition rate was 3.13 pA/msec.

Single channel activity was sometimes observed to occur between cell pairs which, in the light microscope, did not appear to be in contact. Whether the fine filopodia (with gap junctions at their tips) occurred before recording or only formed when the cells were pulled apart (due to manipulator drift) is unknown. On several occasions, cell pairs that were purposely manipulated several cell diameters apart still maintained junctional communication.

Subconductance States

Substates of the mainstate γ_J occurred as momentary shifts in channel conductance during main state events (arrowheads, Fig. 4*A*, *a* and *d*). In addition to this, substates occasionally appeared as steps or flickering during transitional periods of channel opening or closing (arrowheads, Fig. 4*A*, *b*), or as separate channel events of smaller than main γ_J (arrowhead, Fig. 4*A*, *c*).

Substates occurring within main state events as shown in Fig. 4*A*, *a* and *d* were analyzed by calculating each substate as a percent of the main state γ_J within which it was observed. All substate events were pooled from four ATP-loaded cell pairs and grouped into 6 pS bins on a frequency histogram (Fig. 4*B*). The substate frequency distribution was very broad. Events ranged from 3.6–85.6% of the main state with an arithmetic mean 36.8 ± 0.7% (n = 544 events). The non-normalized arithmetic mean was 90.2 ± 2.1 pS (n = 545 events). The mean duration of substate events measured within single level main state

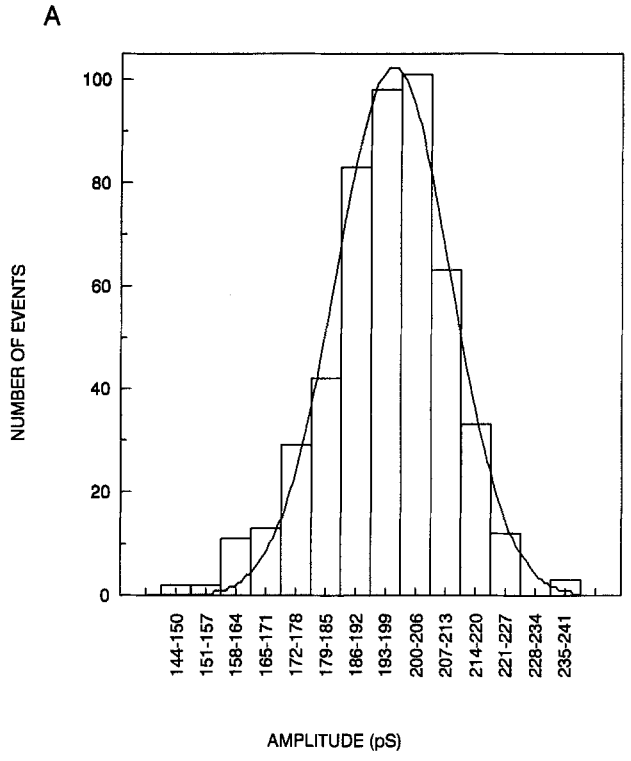

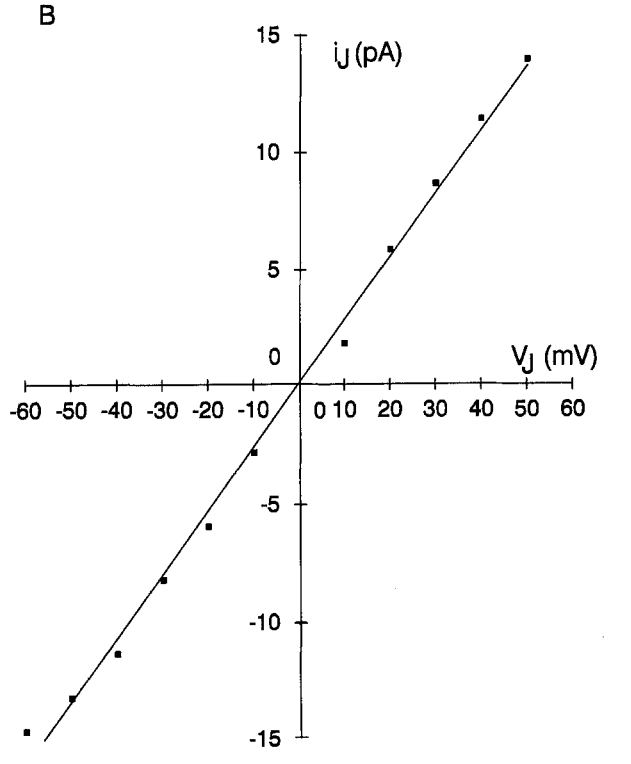

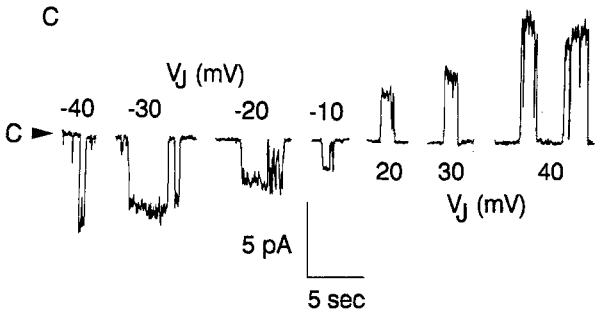

Fig. 3. Main state conductance. (*A*) Frequency histogram of 492 single channel events from one cell pair with ATP in the pipettes. Events were grouped into 7 pS bins and fit with a single Gaussian curve with mean ± SD of 197.21 ± 13.39 pS. V_J was maintained at 20 mV with the cells being held at a range of V_H from −30 to +10 mV. V_H was shifted twice to more depolarized potentials to reduce nonjunctional noise and keep channel activity on scale. (*B*) Dependence of unitary current (i_J) on V_J. One cell of the pair was clamped at 0 mV and the other at a range of voltages between 0 to −60 mV. Channels were not active at depolarized voltages (Fig. 7), therefore the reversal of the single channel current was obtained by alternating the cell maintained at 0 mV. Averaged i_J from 6 cell pairs are graphed against V_J. Single channel events (1–10) were recorded at each V_J. Measurements were made only on single level events. Standard error bars are obscured by data symbols. Results were fit with a regression line with slope 271.0 ± 0.01 pS (r^2 = 0.99) using a linear least-squares method. (*C*) Typical single channel currents are shown for V_J = −40 to +40 mV. Arrowheads denote baseline. Data for figure were sampled from tape at 500 Hz.

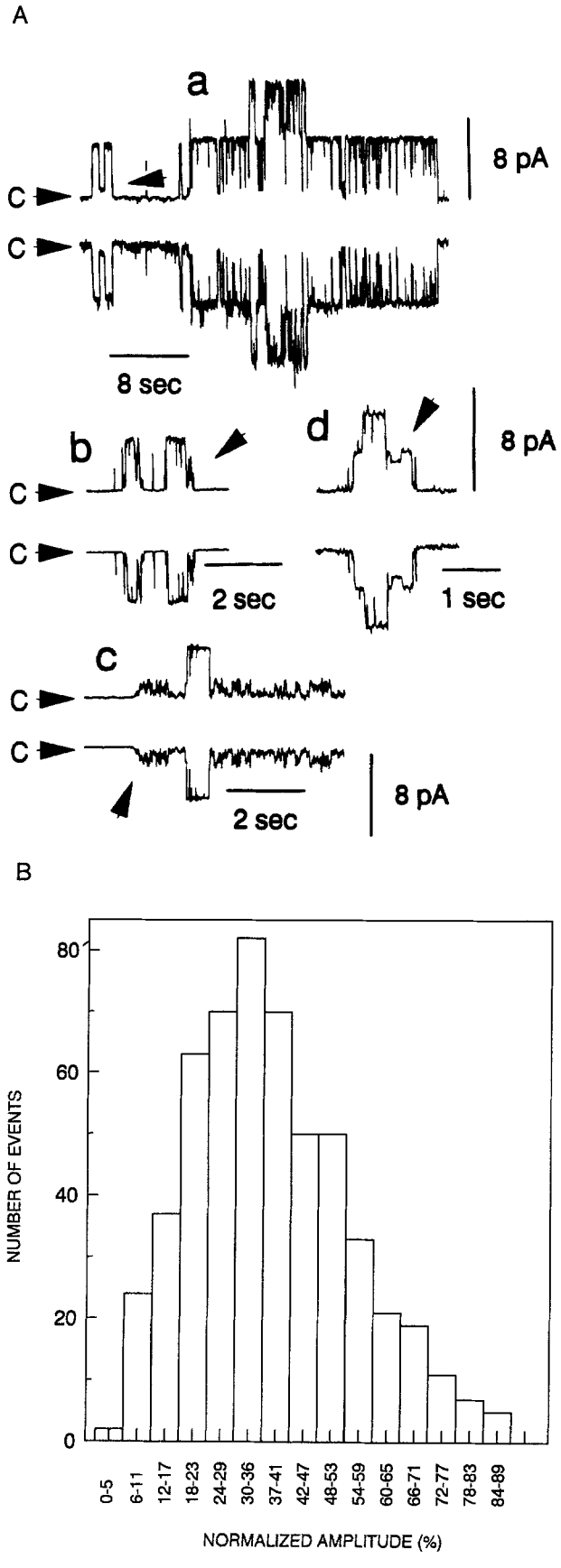

Fig. 4. Substate conductances. (*A*) Examples of single channel events are shown in *a–d*, each from a different cell pair. Current traces from both cells of the pair are shown. Horizontal arrows (*C*) mark the baseline (closed). For *a–c*, V_J = 20 mV; for *d*, V_J = −10 mV. Arrows denote examples of substate events. Substate conductances at the arrows in *a* and *d* were 43 and 235 pS, respectively. Main state conductances for *a–d* were 286, 211, 257, and 305 pS, respectively. *b* is an example of a noisy transition between baseline and main state. Sometimes distinct steps were discerned. *c* is an example of substate behavior that stopped when the channel opened to main state. The data for this figure were sampled from tape 300 Hz. (*B*) Frequency histogram of substate events occurring within main state events (i.e., as in *A a* and *d*). Each event was normalized as a percent of the main state in which it was observed; 544 events from four cell pairs with ATP in the pipette were pooled and grouped into 6 pS bins. The arithmetic mean of substate events was 36.81 ± 0.74% of the main state, ranging from 3.6–85.6% of the main state.

events was 42.1 ± 2.0 msec (n = 536 events) ranging from 4–480 msec. These represent 5.5 ± 0.8% (n = 238 events) of the total open time of all main state events in which main state duration could be estimated. One hundred forty-five of the main state events, often lasting many seconds in duration, did not display substates. If these are removed from the calculation of substate open time then substates represented 14.2 ± 1.6% (n = 93 events) of the main state open time.

The other subconductance behavior of these channels appeared, upon initial visual inspection of the data records, as a smaller conductance channel. This was observed in three separate recordings of short duration (in both ATP-loaded and non-ATP-loaded cell pairs). Upon closer visual inspection, it was observed that the smaller flickering channel activity was not present whenever the larger γ_J channel opened (note the very quiet plateau of the large open channel in Fig 4*A*, *c*). This suggests that only one channel with large main state γ_J was present. The channel flickered between baseline and substate levels and only occasionally opened to the main state. Multiple main state channel openings (concurrent openings) were not observed in these recordings. It is therefore likely that only one or very few channels were active in these cell pairs. In cell pairs in which multiple channels were clearly active, this smaller conductance flickering behavior was never observed, suggesting that this may just be a property of channels in destabilized junctions in very poorly coupled cell pairs. In a one-min recording from one ATP-loaded cell pair, the small conductance activity had a mean conductance of 76.56 ± 3.12 pS (n = 118 events) representing 22% of the 348 ± 6.28 pS (n = 22 events) main state.

V_M Dependence of G_J

The effects of V_M on G_J were examined using the following protocol (Fig. 5*A*). V_H was held at −50 mV for both cells of a pair, and conditioning pulses of the same magnitude (+40 to −90 mV) and duration were supplied to both cells. G_J was monitored by superimposing hyperpolarizing 20 mV test pulses (1 sec, 0.3 Hz) on the conditioning pulses. The test pulses alternated between cells to rule out one-sided artifacts. Conditioning pulse duration was under the experimenter's control so that V_M was changed only when steady-state was reached. G_J was corrected for series resistance errors (*see* Materials and Methods) and by an uncoupling factor which was based on the ratio of the initial G_J at V_M = −50 mV following break-in and G_J at V_M −50 mV just before the conditioning pulse. The long time required to reach each new steady-state caused these experiments to last from 15–30 min allowing substantial uncoupling to occur (Fig. 1*B*).

Figure 5*A* is a sample set of traces showing the effect of V_M on G_J. A conditioning pulse of +40 mV resulted in a decrease in steady-state I_J to near 0 pA with a time course of less than 6 sec. Upon restoration of V_M to −50 mV recovery of steady-state I_J was slow, taking from 18–24 sec. Depolarization to +10 mV in this example resulted in a 30–40% drop in steady-state I_J with a slower time course of 15–18 sec. A −10 mV conditioning pulse resulted in only a slight decrease in steady-state I_J occurring with a slow time course (9–12 sec). In general, the restoration of steady-state I_J upon return of V_M to −50 mV occurred more slowly than the decay with depolarization. The decay and recovery of steady-state I_J was faster and slower, respectively, with larger depolarizing conditioning pulses. Hyperpolarizing conditioning pulses generally resulted in small increases in steady-state I_J with slow time courses (>10 sec). The contribution of nonjunctional currents during conditioning pulses was very small, as seen by the small upward deflections in the overall holding current of both cells with changes in V_M in Fig. 5*A*. This is supported by recordings from single unpaired epidermal cells. The response of single cells to voltage jumps of ±100 mV was ohmic (Fig. 5*C*). The input resistance in 29 single cells was 14.1 ± 2.6 GΩ. These data demonstrate that the nonjunctional membrane, under the conditions used in this study on cell pairs, has very high input resistance and lacks voltage-gated channel activity and, therefore, has minimal effect on the measurement of junctional currents.

The mean steady-state G_J response for seven cell pairs was normalized to the maximal steady-state G_J ($G_{J\max}$) and plotted on a steady-state $G_J/G_{J\max}$ *vs.* V_M curve (Fig. 5*B*). The steady-state G_J curve approached 0 nS at V_M positive to 0 mV and increased sigmoidally at V_M < 0 mV. The mean voltage at half-maximal steady-state G_J was −26.2 ± 4.2 mV (n = 7 cell pairs) ranging from −7.5 to −39 mV. For comparison to similar data from other insect cell pairs, this curve was fit to a previously described two-state Boltzmann relationship for two independent gates in series (Obaid et al., 1983; Verselis et al., 1991),

$$G_J = G_{J\max}/\{1 + \exp[A(V_M - V_o)]\}^2,$$

where $G_{J\max}$ is the maximal steady-state G_J attainable at negative membrane potentials (set to 1), V_o is the V_M at which half the gates are open and A is a constant describing the steepness of the relationship. The data were graphed as $\log[(G_{J\max}/G_J)^{1/2} - 1]$ *vs.* V_M and fit using a linear least-squares method in order to find the best fit values for V_o (V_M at $(G_{J\max}/G_J)^{1/2} - 1 = 1$) and A (slope = $A/2.3$). A curve was generated from the fit values for display (Fig. 5*B*, unbroken line). The fit values for the averaged curve were A = 0.05 and V_o = −5.5 mV (r^2 = 0.83). The best fit values ($r^2 > 0.9$) for the individual curves ranged from 0.047 to 0.083 for A (mean 0.057 ± 0.004) and −22 to +12.7 for V_o (mean −4.81 ± 4.51 mV). The average gating charge was $z = 1.47 \pm 0.11$, determined from $z = ART/F$, where R is the ideal gas constant, T the absolute temperature in degrees Kelvin and F is Faraday's constant. These data suggest that G_J depends strongly on V_M during steady-state conditions.

V_J Dependence of G_J

The effects of V_J on G_J were examined using a voltage protocol in which both cells of the pair were voltage-clamped at −50 mV and one of the cells was stepped through a series of voltage pulses. Square test pulses (30 sec) from +50 to −100 mV in 10 mV increments were randomly applied to one cell generating transjunctional voltages of +100 to −50 mV. Between the test pulses, which were from 30–60 sec apart, the degree of coupling was monitored by applying hyperpolarizing −20 mV pulses (1 sec, 0.3 Hz) alternately to either cell as in the above experiments on V_M dependence. This also allowed monitoring of recovery of I_J from the test pulse to the −50 mV holding potential so that the next test pulse was not applied until a new steady-state was reached. Instantaneous and steady-state G_J (at the beginning and end of the 30 sec test pulse, respectively) was calculated and corrected for R_S errors and for uncoupling as described for G_J *vs.* V_M experiments.

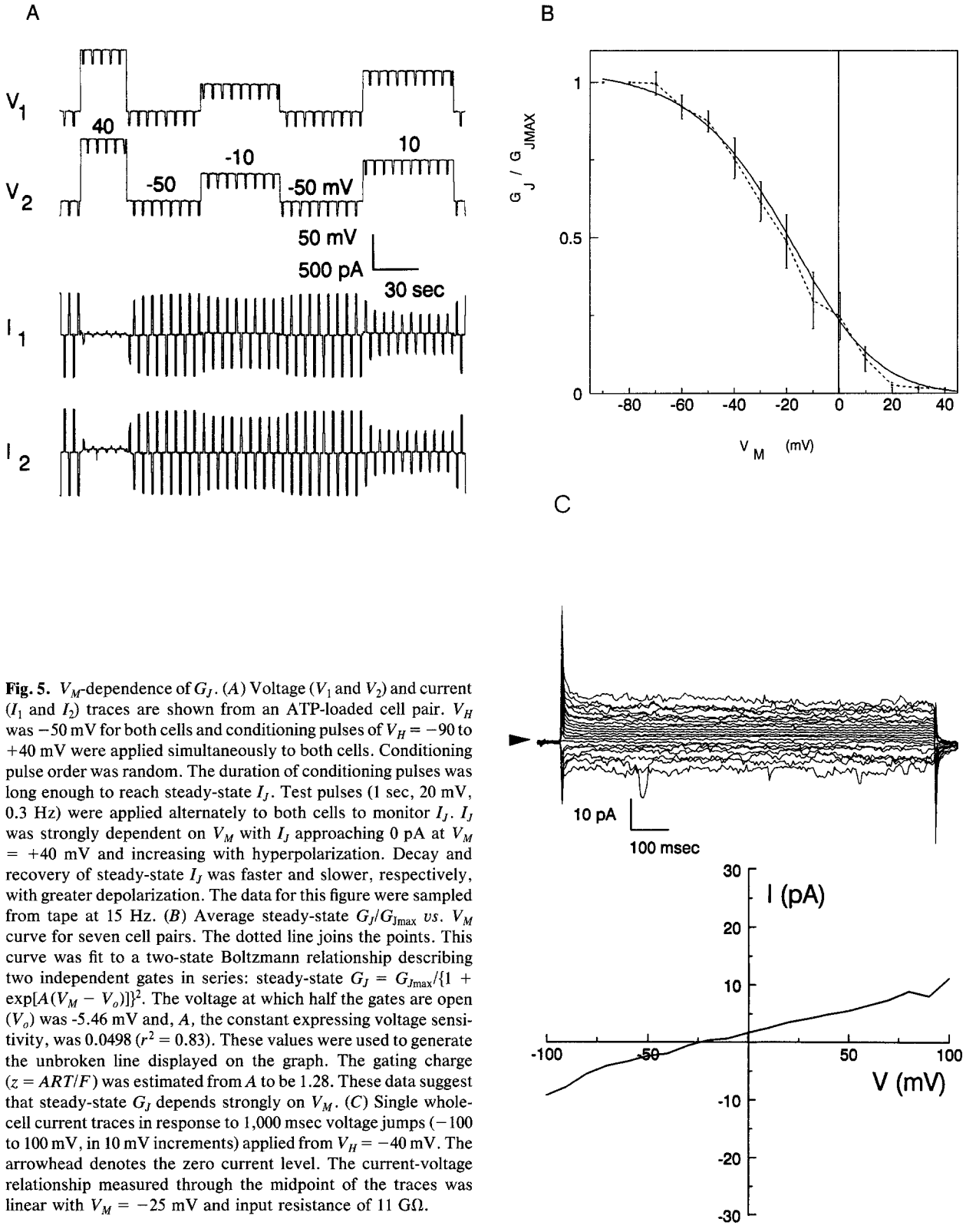

Fig. 5. V_M-dependence of G_J. (*A*) Voltage (V_1 and V_2) and current (I_1 and I_2) traces are shown from an ATP-loaded cell pair. V_H was −50 mV for both cells and conditioning pulses of V_H = −90 to +40 mV were applied simultaneously to both cells. Conditioning pulse order was random. The duration of conditioning pulses was long enough to reach steady-state I_J. Test pulses (1 sec, 20 mV, 0.3 Hz) were applied alternately to both cells to monitor I_J. I_J was strongly dependent on V_M with I_J approaching 0 pA at V_M = +40 mV and increasing with hyperpolarization. Decay and recovery of steady-state I_J was faster and slower, respectively, with greater depolarization. The data for this figure were sampled from tape at 15 Hz. (*B*) Average steady-state G_J/G_{Jmax} *vs.* V_M curve for seven cell pairs. The dotted line joins the points. This curve was fit to a two-state Boltzmann relationship describing two independent gates in series: steady-state $G_J = G_{Jmax}/\{1 + \exp[A(V_M - V_o)]\}^2$. The voltage at which half the gates are open (V_o) was -5.46 mV and, A, the constant expressing voltage sensitivity, was 0.0498 ($r^2 = 0.83$). These values were used to generate the unbroken line displayed on the graph. The gating charge ($z = ART/F$) was estimated from A to be 1.28. These data suggest that steady-state G_J depends strongly on V_M. (*C*) Single whole-cell current traces in response to 1,000 msec voltage jumps (−100 to 100 mV, in 10 mV increments) applied from V_H = −40 mV. The arrowhead denotes the zero current level. The current-voltage relationship measured through the midpoint of the traces was linear with V_M = −25 mV and input resistance of 11 GΩ.

Figure 6*A* shows sample current traces from one cell of a pair at a range of V_J with the V_H = −50 mV for both cells of the pair. The voltage of cell 1 (V_1) was changed during the test pulse. With strongly depolarizing pulses I_J decayed in a time-dependent manner. Decay was faster as depolarization increased. At $V_J = \pm 20$ mV little if any time-dependent decay was observed. At $V_J <$ −30 mV a gradual and very small time-dependent increase in the I_J occurred (15–30 sec; in other cells this time-dependent increase was more pronounced). In this example, even with $V_J >$ +90 mV, there remained a substantial steady-state I_J. In one cell pair in which $V_J >$ +120 mV, a substantial residual steady-state I_J still remained. We found that time-dependent decay of G_J with hyperpolarizing V_J test pulses occurred when the overall holding potential (V_H) was more positive than −50 mV. In Fig. 6*C* an example of junctional currents from one cell of a pair are shown in response to a hyperpolarizing 40 mV V_J test pulse (7.5 sec duration) applied from three different V_H (0, −20, −40 mV). Time-dependent decay in I_J was dependent on the overall V_H of the two cells with increased hyperpolarization decreasing the rate of decay. The same relationship was found for depolarizing V_J test pulses as hyperpolarization of the V_H of both cells decreased the rate of time-dependent decay (*data not shown*).

Both the instantaneous and steady-state G_J were normalized to $G_{J\max}$ (instantaneous and steady-state $G_{J\max}$, respectively) and graphed against V_J. Figure 6*B* plots the average instantaneous and steady-state $G_J/G_{J\max}$ *vs.* V_J curves from seven cell pairs. The instantaneous $G_J/G_{J\max}$ *vs.* V_J curve (Fig. 6*B*) was mostly linear, although a decreasing trend in $G_J/G_{J\max}$ at $V_J > -10$ mV was apparent. This may be due to the difficulty of estimating instantaneous current since the multiple and very slow time constants of the decay made curve-fitting difficult. We instead took maximum I_J as instantaneous I_J. The steady-state $G_J/G_{J\max}$ *vs.* V_J curve (Fig. 6*B*) shows that, as seen in the response to V_M, steady-state G_J increased upon hyperpolarization and decreased with depolarization of one cell. In this case, however, $G_{J\max}$ was reached at about $V_J = 0$ mV followed by a decline at $V_J < -10$ mV. This decrease in steady-state G_J, coupled with the time-dependent decay of I_J with hyperpolarizing V_J test pulses when the overall V_H was greater than −50 mV, suggests the presence of V_J-dependent gating. However, given the asymmetry of the steady-state $G_J/G_{J\max}$ *vs.* V_J curve, the residual steady-state G_J at $V_J >$ 0 mV, and the loss of the time-dependent decay of I_J with hyperpolarizing V_J test pulses when the overall hyperpolarization of both cells was less than −50 mV, V_M is the major voltage dependence determining G_J in these cells.

Voltage Dependence of Single Channel Activity

The effects of voltage on single channel activity were examined using a pair of voltage protocols on cell pairs which had spontaneously uncoupled (ATP-free pipette). In the first protocol, both cells of the pair were clamped at holding voltages between +20 to −20 mV, creating a starting transjunctional voltage of 0 or 20 mV. The potential of only one cell was then hyperpolarized in a staircase of 10 mV steps every 20 sec, thereby increasing V_J with each step. Upon completing this protocol, we began a second one in which both cells were clamped at holding voltages between +20 and −20 mV, creating a transjunctional voltage of 20 mV. Both cells were then hyperpolarized in 10 mV steps, maintaining a constant transjunctional voltage of 20 mV. Because the cell pairs were uncoupling during the recording, the number of active channels was slowly decreasing. Each protocol took 2–3 min with a 1–2 min break in between.

Figure 7*A* shows sample traces from one cell pair. In the top set, only one cell (cell 1) was hyperpolarized in staircase fashion, and in the bottom set both cells were hyperpolarized. When both cells of the pair were at more depolarized voltages, there was little or no channel activity. As either one (top set of traces) or both cells (bottom set of traces) were hyperpolarized, channel activity increased. The open channel probability in relation to cell voltage was estimated by graphing the average NP_o at each voltage level for eight cell pairs (Fig. 7*B*). To determine NP_o (where N is the number of channels and P_o the probability of opening), the mean current (I) during each 20 sec voltage step was calculated by averaging the total current above baseline current and dividing it by i_J, the single channel current level. Each NP_o value was normalized to the maximal NP_o recorded for that cell pair and graphed against the voltage of the most hyperpolarized cell of the pair (V^*). Hyperpolarization of one or both cells resulted in an increase in channel activity (Fig. 7*B*). These data also show that hyperpolarizing membrane potentials affect G_J in well-coupled cells by changing channel activity, with hyperpolarization of both cells increasing channel activity more than if only one cell was hyperpolarized.

Discussion

In this study double, whole-cell patch-clamp methods were used to characterize junctional conduc-

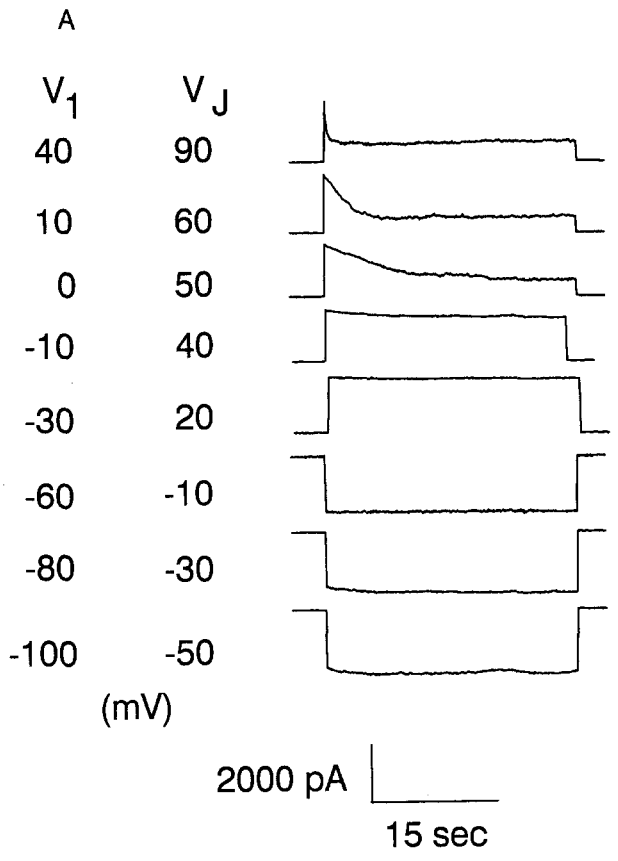

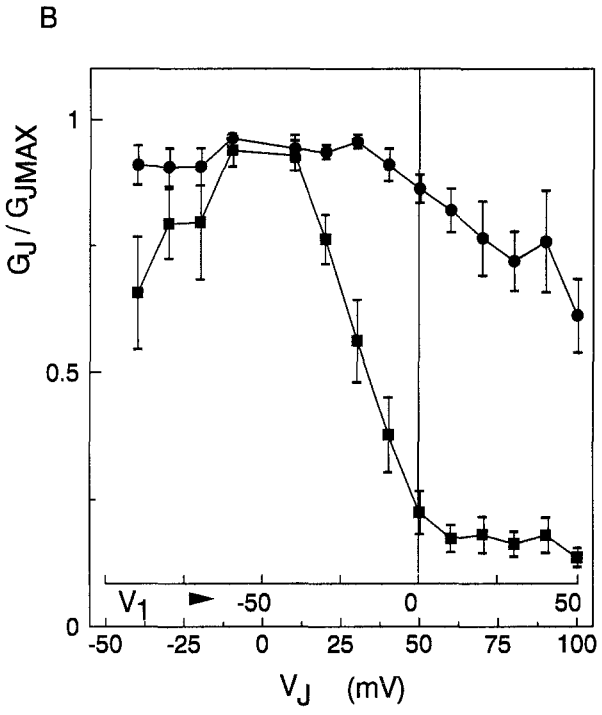

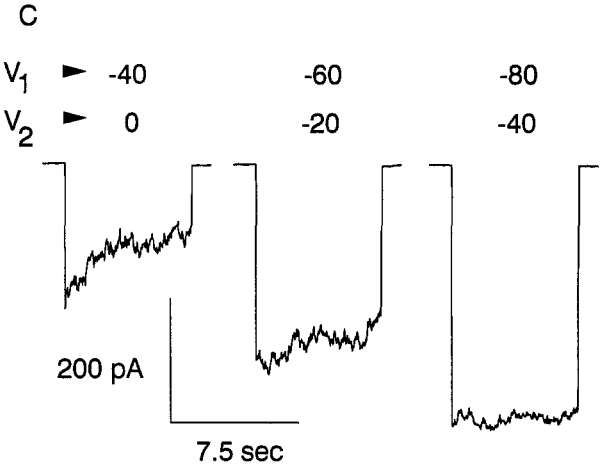

Fig. 6. V_J dependence of G_J. (*A*) Current traces from one cell of a pair with ATP in the pipette solution are shown. V_H was −50 mV for both cells and 30 sec square test pulses were applied to cell 1 (i.e., V_1 = +50 to −100 mV). V_1 and V_J are shown at the left. Depolarizing pulses resulted in time-dependent decay of I_J. Decay was faster the greater the depolarization. At V_J = ±20 mV there was little time-dependent decay in I_J. At V_J < −20 mV often a very slight and gradual time-dependent increase in I_J was evident. At V_J = +90 mV, there was still a large steady-state I_J. (*B*) Average instantaneous and steady-state $G_J/G_{J\max}$ *vs.* V_J curves from seven cell pairs. The instantaneous $G_J/G_{J\max}$ *vs.* V_J curve (●) was nearly linear with a decreasing trend in instantaneous $G_J/G_{J\max}$ at $V_J > -10$ mV. Steady-state G_J (■) decreased with depolarization and increased with hyperpolarization. At $V_J < -10$ mV steady-state $G_J/G_{J\max}$ again decreased suggesting that V_J has some effect on steady-state G_J. The asymmetry of the curve and the residual steady-state G_J at $V_J > 0$ mV suggests that V_M is the stronger determinant of steady-state G_J with changes in V_J. (*C*) Effect of V_H on time-dependent decay of I_J with hyperpolarizing V_J test pulses. V_J test pulses (−40 mV) were applied from V_H = 0, −20 and −40 mV to ATP-loaded cell pairs. V_1 and V_2 during the V_J test pulse are shown at the top of each trace. Increasing hyperpolarization of both cells resulted in the decrease of time-dependent decay in the current and an increase in steady-state I_J. These data suggest that the V_M- and V_J-dependent gates interact, with V_M being the main determinant of G_J.

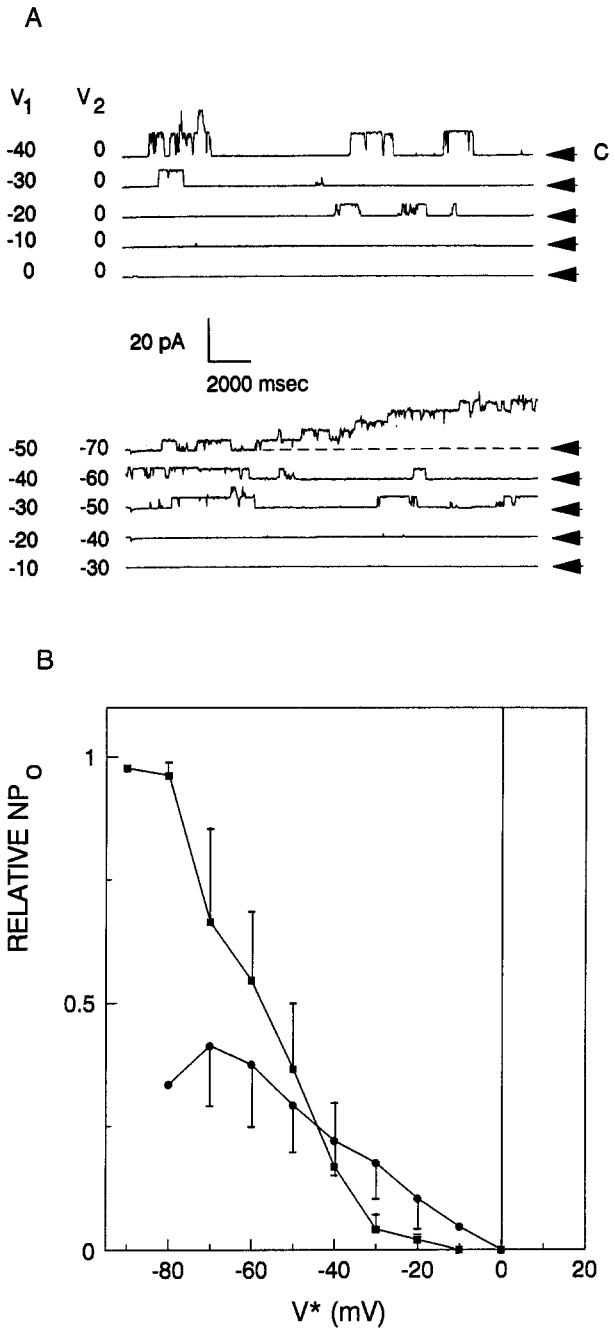

Fig. 7. Voltage dependence of single channel activity. (*A*) Current traces from one cell of a pair without ATP in the pipette solution are shown. The voltages of each cell (V_1 and V_2) are shown at left. The top set of current traces were generated by holding both cells at 0 mV and then hyperpolarizing V_1 in staircase fashion; the voltage dropped by 10 mV with each 20 sec step. The bottom set of traces was generated following the completion of the first set. Here, both cells of the pair were hyperpolarized while maintaining V_J = 20 mV. In both cases, channel activity increased with hyperpolarization. (*B*) Average NP_o *vs.* voltage of most hyperpolarized cell of pair (V^*) for eight cell pairs (normalized to the maximal NP_o for each cell pair). Hyperpolarization of one (●) or both cells (■) of a pair increased channel activity. Pairwise hyperpolarization increased channel activity more than one-sided hyperpolarization.

tances in isolated pairs of insect epidermal cells. ATP- and nonjunctional membrane potential-dependent gating have been described along with the substate gating behavior of a large conductance gap junctional channel.

The range of initial G_J in isolated epidermal cell pairs was 0–95 nS. These values are much lower than that calculated for cell pairs in the intact epidermis. Berdan and Caveney (1985) estimated that there were 15,000 junctional channels between any two cells in the intact *Tenebrio* epidermis. Assuming all of the channels to be open with γ_J = 250 pS, a G_J = 3,750 nS is predicted. As the gap junctions in isolated cell pairs were < 2.5% the size of those in native junctions, extrapolation of the voltage dependence and single channel gating peculiarities described in this study to junctions in the intact epidermis may be limited.

ATP (5 mM) added to the pipette solution stabilized the rapid uncoupling of epidermal cell pairs that occurred during whole-cell recording. A similar ATP-stabilized uncoupling has been described in several vertebrate cell pairs (e.g., Somogyi & Kolb, 1988; Sugiura et al., 1990; Paschke, Eckert & Hülser, 1992) and is attributed to the dialysis of cytoplasm by the pipette solution occurring during recording. The rate of uncoupling is faster in *Tenebrio* compared to vertebrate cell pairs (half-time = 7.6 min *vs.* ~20 min, respectively). Different dialysis rates or differences in the sensitivity of the junctions to the loss of cytoplasmic components may account for this. Since inorganic ions equilibrate in about 3–5 min and the loss of 50% of soluble protein takes about 15 min during whole-cell patch-clamp (Pusch & Neher, 1988), the different kinetics of uncoupling may reflect different dependencies of ATP action on soluble ATP-hydrolyzing proteins such as protein kinases. As ATP clearly plays a major role in stabilizing epidermal gap junctions, we are presently investigating its mechanism of action.

The variation in main state γ_J between epidermal cell pairs was large (197–349 pS, >18 cell pairs). A similar range has been reported for epidermal cell pairs uncoupled with octanol (Churchill & Caveney, 1993*b*). This could indicate the occurrence of different channels with different γ_J or the ability of one channel type to assume different conductance states. In addition to the observation of only one main state γ_J per cell pair, all other characteristics of the observed channels were the same including: the pattern of opening, transition times, substate behavior, and voltage and ATP dependence. It is also possible that only one channel type with the same γ_J was observed in all cell pairs. In this case, cell-to-cell variability could instead be attributed to

errors in estimating the effective transjunctional voltage at the junction because of series or cytoplasmic resistance errors (Wilders & Jongsma, 1992) or, space clamp problems arising in the region of gap junctions occurring at the end of fine filopodia. We have calculated the errors due to series resistance to be $\ll$10%. Space clamp errors would be difficult to estimate. However, it is unlikely that filopodia cause a problem since we have never observed obvious changes in γ_J that might arise due to filopodia formation with manipulator drift during recording in one cell pair. Gap junctions at the end of filopodia in other cell types have been described (Loewenstein, Kanno & Socolar, 1978; Rook et al., 1988).

Large conductance gap junctional channels have been described for three insect cell types. Apart from the epidermal channel, γ_J of 345 pS in cockroach hemocytes (Churchill et al., 1993) and 133 pS in a mosquito cell line (Bukauskas et al., 1991) have been reported. In one other invertebrate (earthworm giant axon) in which single channel conductance has been examined 30–40 pS and 90–110 pS have been reported (Brink & Fan, 1989). In vertebrates more than 80% of the reported γ_J are below 100 pS (e.g., Neyton & Trautmann, 1985; Burt & Spray, 1988; Rook et al., 1988; Somogyi & Kolb, 1988; Veenstra & DeHaan, 1988; McMahon, Dowling & Knapp, 1989; Dermeitzel et al., 1991; Giaume et al., 1991; Moore, Beyer & Burt, 1991; Spray et al., 1991*b*; Paschke, et al., 1992) and only a few γ_J between 100–200 pS have been reported (e.g., Neyton & Trautmann, 1985; Chow & Young, 1987; Somogyi & Kolb, 1988; Veenstra & DeHaan, 1988). Only those in embryonic chick heart and lens are in the 200–300 pS range (Chen & DeHaan, 1992; Miller, Zampighi & Hall, 1992). The generally larger γ_J of insect *vs.* vertebrate cells is consistent with the findings of larger pore sizes in insects. Previous experiments with fluorescent tracer molecules have demonstrated the apparent limiting pore size in *Chironomus* salivary gland junctions to be between 2 and 3 nm corresponding to a molecular weight cut-off of 1,200–2,450 D (Flagg-Newton et al., 1979; Schwarzmann et al., 1981; Zimmerman & Rose, 1985). In contrast, junctions in cultured mammalian cells have a 1.6–2 nm pore size and 900–1000 D cut-off (Flagg-Newton et al., 1979; Schwarzmann et al., 1981).

Three types of substate behavior were observed in the epidermis. These included: (i) a broad range of partially closed states that occurred during main state events; (ii) flickering or distinct steps that occurred during opening and closing transitional periods of main state events; and (iii) flickering between the fully closed state and the substate interrupted by occasional complete openings to the main state. Following the substate criteria outlined by Fox (1987), these would be substates of the main state channel, since substates occurred infrequently, interconverting directly with the main state, and when occurring as apparent independent events, were always observed in the presence of, but not at exactly the same time, as main state activity. The suggestion that gap junctional channels can assume substates is not new (Neyton & Trautmann, 1985; Veenstra & DeHaan, 1986, 1988; Somogyi & Kolb, 1988). It is unclear whether the conductance levels observed in these reports represented substates or the activity of different populations of channels. Evidence in a recent report strongly suggests the presence of voltage-dependent substates in chick heart gap junctions (Chen & DeHaan, 1992).

Slow transition times for opening and closing of the main state epidermal channel were observed (1–28 msec). It was difficult to measure transition times at sample frequencies faster than 5 kHz because of increases in background noise. Although the 5 kHz sample frequency would be expected to slow the measured transition times, transitions $>$ 15 msec would still represent very slow (msec) transitions at faster sample frequencies. Most nonjunctional ion channels and some gap junctional channels (Veenstra & DeHaan, 1988) have fast transition times (μsec), reflecting the instability of the channel in any other but the opened and closed conformations. The slow transition times of epidermal and some other gap junctional channels (Neyton & Trautmann, 1985; Chow & Young, 1987; Rook et al., 1988; Rüdisüli & Weingart, 1989) suggest that these may have multiple stable conformations and hence can transit through those states more slowly. The observation of slow transition times, coupled with the multiplicity of substate conductances and flickering transitional gating properties in epidermal channels, support a model of gating which states that gap junctional channels can open to any conductance between zero and their fully open state but usually have two or more preferential conducting states (Neyton & Trautmann, 1985; Rook et al., 1988; Young, Cohn & Gilula, 1987).

G_J in *Tenebrio* gap junctions is strongly dependent on V_M. A similar dependence has been reported in gap junctions in three other insect tissues, *Chironomus* (Obaid et al., 1983) and *Drosophila* salivary gland cell pairs (Verselis & Bargiello, 1991; Verselis et al., 1991), and *Aedes albopictus* cultured cells (Bukauskas, et al., 1991). In all examples, G_J increased sigmoidally with hyperpolarization and approached zero with depolarization. The V_M at half-maximal conductance in *Tenebrio* was -26 mV. As

this lies within the normal range of membrane potential in the intact epidermis (Caveney & Blennerhassett, 1980), V_M could play a role in controlling the overall tone of junctional conductance. There is reason, however, for caution in making this extrapolation from whole-cell patch-clamped cell pairs to intact tissue with thousands of gap junction channels per cell. Obaid et al. (1983) have clearly demonstrated in *Chironomus* that cytoplasmic conditions affecting pH and pCa^{2+} determine V_o of the V_M-dependent response, suggesting that internal perfusion of cytoplasm during patch clamp could affect the measurement of V_o. In addition, Jongsma et al. (1990) have suggested that the size of gap junction plaques may affect the proportion of the electric field sensed by each channel, thereby explaining the loss of voltage dependence in large *vs.* small gap junctions in mammalian heart.

V_M dependence was suggested to be the primary means of voltage control in *Chironomus* cell pairs (Obaid et al., 1983). In *Drosophila* (Verselis & Bargiello, 1991; Verselis et al., 1991) and *Aedes*, however, both V_M and V_J dependence were found. In both cell types strongly depolarizing and hyperpolarizing V_J pulses resulted in a time-dependent decay in I_J. In addition, the steady-state G_J *vs.* V_J curve was bell-shaped but asymmetric about 0 mV, supporting the suggestion that both V_J- and V_M-dependent gating mechanisms were operative during V_J pulses. A similar response was observed in *Tenebrio* cell pairs. In *Tenebrio*, time-dependent decay in G_J only occurred in response to hyperpolarizing V_J test pulses when $V_H \leq -40$ mV, suggesting that the V_M- and V_J-dependent gates interact. Kinetic analyses, as have been done in *Drosophila* to demonstrate the presence and interaction of both V_J- and V_M-dependent gates (Verselis & Bargiello, 1991; Verselis et al., 1991), must be done to differentiate between the contributions of these two mechanisms in determining epidermal cell G_J.

Our long-term goal in examining patch-clamped epidermal cell pairs is to gain insight into the complex gating mechanisms and unique permselective properties of insect gap junctions that may be important during development. In addition, the presence of strong V_M- and ATP-dependent gating mechanisms in the epidermis suggests that the large conductance gap junctional channels appear capable of assuming multiple subconductance states. These channel substates may have different relative permeability (permselectivity) to inorganic and organic ions. This might explain how junctional permeability to inorganic ions and fluorescent tracers may change selectively in the segmented epidermis and at segment borders during development (Caveney & Safranyos, 1989). Junctional permselectivity could result from changes in the relative amounts of distinct channel types with different permeability properties or, as favored by this study, the option of a single channel type with different substate permeabilities. If it could be demonstrated that substates had permeabilities distinct from the main state and were subject to differential regulation, then we would be one step closer to defining a role for gap junctions in insect development. Future patch-clamp studies of cells isolated from different regions of the epidermis, or exposed to metabolic intermediates in the patch pipettes, may help unravel the complexities of junctional communication in this tissue.

We gratefully acknowledge the helpful advice of Dr. Stephen Sims. This work was supported by NSERC of Canada grant No. A6797 to S.C. D.C. was supported by an NSERC scholarship for part of this work.

References

Bennett, M.V.L., Barrio, L.C., Bargiello, T.A., Spray, D.C. 1991. Gap junctions: new tools, new answers, new questions. *Neuron* **6**:305–320

Berdan, R.C., Caveney, S. 1985. Gap junction ultrastructure in three states of conductance. *Cell. Tissue. Res.* **239**:111–122

Blennerhassett, M.G., Caveney, S. 1984. Separation of developmental compartments by a cell type with reduced junctional permeability. *Nature* **309**:361–364

Brink, P.R., Fan, S.-F. 1989. Patch clamp recordings from membranes which contain gap junction channels. *Biophys. J.* **56**:579–593

Bukauskas, F., Kempf, C., Weingart, R. 1991. Electrical coupling between cells of the insect *Aedes albopictus*. *J. Physiol.* **448**:321–337

Burt, J.M., Spray, D.C. 1988. Single-channel events and gating behaviour of the cardiac gap junction channel. *Proc. Natl. Acad. Sci. USA* **85**:3431–3434

Caveney, S. 1978. Intercellular communication in insect development is hormonally controlled. *Science* **199**:192–195

Caveney, S. 1985. The role of gap junctions in development. *Annu. Rev. Physiol.* **47**:319–335

Caveney, S., Berdan, R.C., McLean, S. 1980. Cell-to-cell ionic communication stimulated by 20-hydroxyecdysone occurs in the absence of protein synthesis and gap junction growth. *J. Insect Physiol.* **26**:557–567

Caveney, S., Blennerhassett, M.G. 1980. Elevation of ionic conductance between insect epidermal cells by β-ecdysone *in vitro*. *J. Insect Physiol.* **26**:13–25

Caveney, S., Safranyos, R.G.A. 1989. Developmental physiology of insect epidermal gap junctions. *In:* Cell Interactions and Gap Junctions. N. Sperelakis, and W.C. Cole, editors. V.1, pp. 107–123. CRC, Boca Raton, FL

Chen, Y.-H., DeHaan, R.L. 1992. Multiple-channel conductance states and voltage regulation of embryonic chick cardiac gap junctions. *J. Membrane Biol.* **127**:95-111

Chow, I., Young, S.H. 1987. Opening of single gap junction channels during formation of electrical coupling between embryonic muscle cells. *Dev. Biol.* **122**:332–337

Churchill, D., Caveney, S. 1993a. Double whole-cell patch-clamp of gap junctions in insect epidermal cell pairs: single channel conductance, voltage dependence, and spontaneous uncoupling. *In:* Gap Junctions. J.E. Hall, G.A. Zampighi, and R.M. Davis, editors. pp. 239–245. Elsevier, Amsterdam

Churchill, D., Caveney, S. 1993b. Isolation of epidermal cell pairs from an insect, *Tenebrio molitor*, for dual whole-cell recording of large conductance gap junctional channels. *J. Exp. Biol.* **178:**261–267

Churchill, D., Coodin, S., Shivers, R.R., Caveney, S. 1993. Rapid de novo formation of gap junctions between insect hemocytes *in vitro*: A freeze-fracture, dye-transfer and patch-clamp study. *J. Cell Sci.* **104:**763–772

Dermietzel, R., Hertzberg, E.L., Kessler, J.A., Spray, D.C. 1991. Gap junctions between cultured astrocytes: immunocytochemical, molecular, and electrophysiological analysis. *J Neurosci.* **11:**1421–1432

Flagg-Newton, J., Simpson, I., Loewenstein, W.R. 1979. Permeability of the cell-to-cell membrane channels in mammalian cell junction. *Science* **205:**404–407

Fox, J.A. 1987. Ion channel subconductance states. *J. Membrane Biol.* **97:**1–8

Giaume, C. 1991. Application of the patch-clamp technique to the study of junctional conductance. *In:* Biophysics of Gap Junction Channels. C. Peracchia, editor. pp. 175–190. CRC, Boca Raton, FL

Giaume, C., Kado, R.T., Korn, H. 1987. Voltage-clamp analysis of a crayfish rectifying synapse. *J. Physiol.* **386:**91–112

Giaume, C., Fromaget, C., Aoumari, A.E., Cordier, F., Glowinski, J., Gros, D. 1991. Gap junctions in cultured astrocytes: single-channel currents and characterization of channel-forming protein. *Neuron* **6:**133–143

Guthrie, S.C., Gilula, N.B. 1989. Gap junctional communication and development. *Trends Neurosci.* **12:**12–16

Jongsma, H.J., Wilders, R., van Ginneken, A.C.G., Rook, M.B. 1990. Modulatory effect of the transcellular electric field on gap junction conductance. *In:* Biophysics of Gap Junction Channels. C. Peracchia, editor. pp.175-190. CRC, Boca Raton, FL

Loewenstein, W.R. 1981. Junctional intercellular communication. The cell-to-cell membrane channel. *Physiol. Rev.* **61:**829–913

Loewenstein, W.R., Kanno, Y., Socolar, S.J. 1978. Quantum jumps of conductance during formation of membrane channels at cell-cell junction. *Nature* **274:**133–136

McMahon, D.G., Knapp, A.G., Dowling, J.E. 1989. Horizontal cell gap junctions: single-channel conductance and modulation by dopamine. *Proc. Natl. Acad. Sci. USA* **86:**7639–7643

Miller, A.G., Zampighi, G.A., Hall, J.E. 1992. Single-membrane and cell-to-cell permeability properties of dissociated embryonic chick lens cells. *J. Membrane Biol.* **128:**91–102

Moore, L.K., Beyer, E.C., Burt, J.M. 1991. Characterization of gap junction channels in A7r5 vascular smooth muscle cells. *Am. J. Physiol.* **260:**C975–C981

Neyton, J., Trautmann, A. 1985. Single-channel currents of an intercellular junction. *Nature* **317:**331–335

Neyton, J., Trautmann, A. 1986. Acetylcholine modulation of the conductance of intercellular junctions between rat lacrimal cells. *J. Physiol.* **377:**283–295

Obaid, A.L., Socolar, S.J., Rose, B. 1983. Cell-to-cell channels with two independently regulated gates in series: analysis of junctional conductance modulation by membrane potential, calcium, and pH. *J. Membrane Biol.* **73:**69–89

Paschke, D., Eckert, R., Hülser, D.F. 1992. High-resolution measurements of gap-junctional conductance during perfusion with anti-connexin antibodies in pairs of cultured mammalian cells. *Pfluegers Arch.* **420:**87–93

Pusch, M., Neher, E. 1988. Rates of diffusional exchange between small cells and a measuring patch pipette. *Pfluegers Arch.* **411:**204–211

Rook, M.B., Jongsma, H.J., van Ginneken, A.C.G. 1988. Properties of single gap junctional channels between isolated neonatal rat heart cells. *Am. J. Physiol.* **255:**H770–H782

Ruangvoravat, C.P., Lo, C.W. 1992. Restrictions in gap junctional communication in the *Drosophila* larval epidermis. *Dev. Dynamics* **193:**70–82

Rüdisüli, A., Weingart, R. 1989. Electrical properties of gap junction channels in guinea-pig ventricular cell pairs revealed by exposure to heptanol. *Pfluegers Arch.* **415:**12–21

Schwarzmann, G., Wiegandt, H., Rose, B., Zimmerman, A., Ben-Haim, D., Loewenstein, W.R. 1981. Diameter of the cell-to-cell junctional membrane channels as probed with neutral molecules. *Science* **213:**551–553

Somogyi, R., Kolb, H.A. 1988. Cell-to-cell channel conductance during loss of gap junctional coupling in pairs of pancreatic acinar and Chinese hamster ovary cells. *Pfluegers Arch.* **412:**54–65

Spray, D.C., Bennett, M.V.L. 1985. Physiology and pharmacology of gap junctions. *Annu. Rev. Physiol.* **47:**281–303

Spray, D.C., Bennett, M.V.L., Campos de Carvalho, A.C., Eghbali, B., Moreno, A.P., Verselis, V. 1991*a*. Transjunctional voltage dependence of gap junction channels. *In:* Biophysics of Gap Junction Channels. C. Peracchia, editor. pp. 175–190. CRC, Boca Raton, FL

Spray, D.C., Chanson, M., Moreno, A.P., Dermietzel, R., Meda, P. 1991*b*. Distinctive gap junction channel types connect WB cells, a clonal cell line derived from rat liver. *Am. J. Physiol.* **260:**C513–C527

Sugiura, H., Toyama, J., Tsuboi, N., Kamiya, K., Kodama, I. 1990. ATP directly affects junctional conductance between paired ventricular myocytes isolated from guinea pig heart. *Circ. Res.* **66:**1095–1102

Veenstra, R.D. 1990. Voltage-dependent gating of gap junction channels in embryonic chick ventricular cell pairs. *Am. J. Physiol.* **258:**C662–672

Veenstra, R.D., DeHaan, R.L. 1986. Measurement of single channel currents from cardiac gap junctions. *Science* **233:**972–974

Veenstra, R.D., DeHaan, R.L. 1988. Cardiac gap junction channel activity in embryonic chick ventricle cells. *Am. J. Physiol.* **254:**H170–180

Verselis, V.K., Bargiello, T.A. 1991. Dual voltage control in a *Drosophila* gap junction channel. *In:* Biophysics of Gap Junction Channels. C. Peracchia, editor. pp. 117–129. CRC, Boca Raton, FL

Verselis, V.K., Bennett, M.V.L., Bargiello, T.A. 1991. A voltage-dependent gap junction in *Drosophila melanogaster*. *Biophys. J.* **59:**114–126

Wang, H.-Z., Li, J., Lemanski, L.F., Veenstra, R.D. 1992. Gating of mammalian cardiac gap junction channels by transjunctional voltage. *Biophys. J.* **63:**139–151

Warner, A.E., Lawrence, P.A. 1982. Permeability of gap junctions at the segmental border in insect epidermis. *Cell* **28:**243–252

Wigglesworth, V.B. 1984. The integument. *In:* Insect Physiology. pp. 1–17. Chapman and Hall, New York

Wilders, R., Jongsma, H.J. 1992. Limitations of the dual voltage

clamp method in assaying conductance and kinetics of gap junction channels. *Biophys. J.* **63**:942–953

Wolpert, L. 1978. Gap junctions: channels for communication in development. *In:* Intercellular Junctions and Synapses. J. Feldman, N.B. Gilula and J.D. Pitts, editors. pp. 79-96. Chapman and Hall, London

Young, J.D.-E., Cohn, Z.A., Gilula, B. 1987. Functional assembly of gap junction conductance in lipid bilayers: Demonstration that the major 27 kd protein forms the junctional channel. *Cell* **48**:733–743

Zimmerman, A.L., Rose, B. 1985. Permeability properties of cell-to-cell channels: kinetics of fluorescent tracer diffusion through a cell junction. *J. Membrane Biol.* **84**:269–283

Note Added in Proof

In a recent short communication Bukauskas and Weingart (1993) have reported a large conductance mosquito gap junctional channel having subconductance states of 1/5 and 1/7 of the 365 pS main conductance state.